Sparse Wave Packets Discriminate Motor Tasks in EEG–based BCIs

Carlos A. Loza[1] and Jose C. Principe[2]

Abstract— We propose a novel non–linear source separation technique for single–channel, multi–trial Electroencephalogram (EEG). First, a generative model is posited as the generating process behind bandpassed traces. In particular, the inputs are conceived as the state variable of a switching mechanism that samples temporal snippets from two distributions corresponding to a background component and a phasic event or wave packet counterpart. In order to non–linearly separate the sources, we propose a neurophysiologically principled, non–linear mapping to a space of ℓ_2–norms via the Embedding Transform. In this way, the estimated phasic event component— an ideal time series where neuromodulations are emphasized— is isolated for further processing. The algorithm is tested on the Brain–Computer Interface (BCI) Competition 4 dataset 2a. The results not only surpass classic power–based measures, but also highlight the discriminative nature of scale–specific wave packets in motor imagery tasks. The inherent switching mechanism that generates the traces suggests a transient, temporally sparse feature of the neuromodulations that can be further exploited in applications where compression is advantageous.

Index Terms— BCI, EEG, Embedding Transform, Wave Packets

I. INTRODUCTION

The Electroencephalogram (EEG) constitutes a key mesoscopic signature of the brain. Specifically, scale–specific events are the result of spatio–temporal synchronization of neuronal assemblies at different topographical levels or recruitment densities [1]. These temporal patterns are inherently transient due to energy constraints and the need of fine multi–scale, time–dependent encoding of internal physiological processes or external stimuli. Examples of relevant EEG–based applications include sleep scoring [2], epilepsy studies [3], prediction in Parkinson's disease [4], and Brain–Computer Interfaces (BCI) [5].

EEG–based BCIs provide a suitable non–invasive alternative to model encoding and decoding mechanisms in the brain without the inherent risks associated to surgical procedures. In particular, paralyzed or locked in patients have successfully utilized this type of BCIs for cursor control, computer communication and wheelchair control via voluntary modulation of oscillatory rhythms during sensory–related tasks [6], [7], [5]. For instance, slow cortical potentials and the mu (8–12 Hz) and beta (18–26 Hz) rhythms have been associated to prediction and discrimination of motor imagery tasks [8], [9]. Such systems are anchored on the neurophysiological principles of event–related synchronization (ERS) and desynchronization (ERD) in the EEG [10].

The EEG reflects the dynamics and fractal nature of its generating structure. The brain features distinctive perpetual transitions over time—from complex, unpredictable chaos to robust, briefly predictable epochs. Likewise, the EEG displays ceaseless shifts between temporally uncorrelated activity and organized, correlated signatures in the form of transient patterns over time [1]. In dynamical systems, such behavior is known as criticality: a type of stability where the network reorganizes its dynamics back and forth due to perturbations (either internal, e.g. physiological processes, or external, e.g. sensory stimuli) [11]. The challenge of quantitative EEG analysis is to discriminate between modes in a principled manner and find pertinent behavioral correlates.

Early attempts at mode discrimination estimated the Power Spectral Density of the EEG in order to model the spectral distribution of the sources; yet, such approaches completely disregard the phase of the input, i.e. temporal information was lost. Then, Time–Frequency decompositions incorporated a time component to the modeling framework with the Short–Time Fourier Transform and Wavelet analysis (for a detailed review, see [12]); however, the temporal segmentation, i.e. choice of window parameter, is still an open subject and application–dependent problem [13], [14].

We propose a non–linear source separation method for the bandpassed EEG where neurophysiological principles are exploited in order to isolate snippets that discriminate motor tasks in multi–channel BCIs. The framework relies on the features of the EEG dynamics to estimate a threshold that isolates the unorganized activity (i.e. a background component) from the relevant spatio–temporal signatures, also known as *wave packets* (a term coined by Freeman [12]). We exploit the Embedding Transform to non–linearly map the inputs to a surrogate space where both modes can be separated [15]. The proposed single–parameter algorithm is completely data–driven, does not rely on add–hoc thresholds, and, unlike spectral estimation methods, features exceptional temporal resolution. We test the algorithm on the publicly available BCI Competition 4 Dataset 2a with promising results that not only highlight the plausibility of the framework, but also reveal the temporally sparse nature of scale–specific wave packets in the EEG. The paper continues as follows: Section 2 details the rationale behind the Discriminant Embedding Transform alongside its practical implementation. Section 3 describes the experimental results, and lastly, Section 4 concludes the paper and discusses further work.

[1]Carlos A. Loza is with the Department of Mathematics, Universidad San Francisco de Quito, Quito, Ecuador `cloza@usfq.edu.ec`

[2]Jose C. Principe is with the Computational NeuroEngineering Laboratory (CNEL), University of Florida, Gainesville, FL `principe@cnel.ufl.edu`

II. THE DISCRIMINATIVE EMBEDDING TRANSFORM

Let $\tilde{y}[n]$ be a bandpassed, single–channel, single–trial EEG trace that can be separated in two components:

$$\tilde{y}[n] = y[n] + z[n] \tag{1}$$

where $y[n]$ is the ideal, noiseless time series that contains scale–specific reoccurring patterns (neuromodulations or wave packets), i.e. a phasic event component, and $z[n]$ is the ongoing, spontaneous EEG activity—a background component. $\tilde{y}[n]$ can be conceived as the output of a switching mechanism that samples snippets from two generating distributions according to a phasic event rate. Long–standing theories regarding event–related potential (ERP) generation support the presence of two components in the EEG, i.e. stimulation elicits a response from neuronal populations that is both additive and independent from ongoing activity [16].

Mode separation is possible only if additional constraints are imposed. In particular, the experimental findings of Walter J. Freeman are harnessed here [12]. If the original, unfiltered version of $\tilde{y}[n]$ is the state variable of a generating network at rest, the amplitudes will resemble a Gaussian distribution (± 3 standard deviations). If on the other hand, the network shifts toward an active state, the resulting raw EEG amplitudes deviate from Gaussianity according to higher–order moments. Moreover, if $\tilde{y}[n]$ is the result of linear filtering, the Gaussian/Non–Gaussian regimes are preserved according to the state of the network.

In [15], the Embedding Transform was proposed as a modeling approach of both modes. A bandpassed, single–channel, N–sample–long, EEG trace, $\tilde{y}_k[n]$, from a set of T trials is non–linearly mapped to a surrogate space of constrained ℓ_2–norms, $\beta_M^{(k)}$:

$$\beta_M^{(k)} = ||\tilde{y}_k[\pi_i - M/2 : \pi_i + M/2]||_2 \tag{2}$$
$$\text{s.t.} \quad \pi_i \in \Pi$$

where M is the embedding parameter (in samples) and Π is the set of middle–points of all potential non–overlapping windows of length M in $\tilde{y}_k[n]$. Unlike classic embeddings where M–sample–long windows are slided over the input, the Embedding Transform builds the set Π in a sequential scheme: the algorithm starts by isolating the indices where relevant modulatory activity is present (exploiting the smoothed instantaneous amplitude of the analytic signal). Lastly, the indices corresponding to the remaining unmodulated snippets complete the set Π. Algorithm 1 details the non–linear mapping for a single EEG recording. For multi–trial experiments, the final set of ℓ_2–norms is equal to:

$$\beta_M = \bigcup_{k=1}^{T} \beta_M^{(k)} \tag{3}$$

The Embedding Transform maps the snippets from $z[n]$ to a chi–distribution with M degrees of freedom in the β_M space; furthermore for large embeddings, this density defaults to a Gaussian distribution by the Central Limit Theorem. On the other hand, snippets from the phasic event component are mapped to a second mode in β_M. Separability can be achieved via higher–order moments (see [17]); however, we opt for a parametric fitting of a Gaussian mixture with 2 components where the threshold is equal to:

$$\gamma = \mu_Z + 3\sigma_Z \tag{4}$$

where μ_Z and σ_Z are the mean and standard deviation of the Gaussian corresponding to the background component in the β_M space. In summary, the Discriminative Embedding Transform non–linearly estimates $\hat{y}_k[n]$ such that its M–sample–long snippets are larger than the threshold, γ:

$$\hat{y}_k[n] = \sum_i \tilde{y}_k[\pi_i - M/2 : \pi_i + M/2] \tag{5}$$
$$\text{s. t.} \quad ||\tilde{y}_k[\pi_i - M/2 : \pi_i + M/2]||_2 \geq \gamma$$

The estimated phasic event trace, $\hat{y}_k[n]$, is a collection of potential M–sample–long wave packets (M–snippets) that can be utilized on further analysis, inference and discriminative frameworks. The only parameter, M, must be set based on Neurophysiology and, more specifically, according to the scale under analysis, i.e. oscillatory EEG rhythm of study.

Fig. 1 illustrates the density estimation of β_M and the corresponding thresholds for the 9 subjects of the BCI Competition 4 dataset 2a. γ effectively delineates the separation between modes (background component to the left and phasic event component to the right). In general, the distributions have positive skewness, which suggests a high density of spontaneous activity and a low probability of high–amplitude M–snippets, i.e. relevant wave packets have a transient and temporally sparse nature. Consequently, the Discriminative Embedding Transform performs a non–linear, neurophysiologically principled filtering of the inputs where only a small fraction of the samples are preserved.

Algorithm 1 Embedding Transform.

Input: $\tilde{y}_k[n]$, M
Output: $\beta_M^{(k)}$

$\beta_M^{(k)} \leftarrow \emptyset$
$r[n] \leftarrow \mathbf{1}_{N \times 1}$
$y'[n] = \text{envelope}(\tilde{y}_k[n])$
$s[n] = \text{smooth}(y'[n], M)$
$\{\zeta_i\}_{i=1}^p = \text{peaks}(s[n], M)$
{Begin with potential modulated patterns}
for $i = 1, \ldots, p$ **do**
$\quad \beta_M^{(k)} \leftarrow \beta_M^{(k)} \cup ||\tilde{y}_k[\zeta_i - M/2 : \zeta_i + M/2]||_2$
$\quad r[\zeta_i - M/2 : \zeta_i + M/2] = \mathbf{0}_{M \times 1}$
end for
{Proceed with non–modulated patterns until exhaustion}
$\{\zeta_i\}_{i=1}^p \leftarrow \text{findMsnippets}(r[n], M)$
if $\zeta \neq \emptyset$ **then**
$\quad$ **for** $i = 1, \ldots, p$ **do**
$\quad \quad \beta_M^{(k)} \leftarrow \beta_M^{(k)} \cup ||\tilde{y}_k[\zeta_i - M/2 : \zeta_i + M/2]||_2$
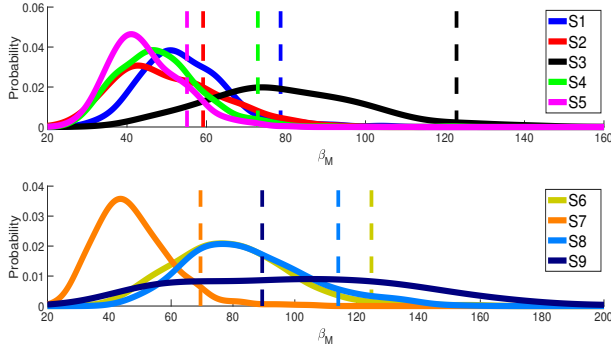$\quad$ **end for**
end if

Fig. 1. β_M distributions after the Embedding Transform. Vertical lines show estimated thresholds, γ. SX denotes Subject X in BCI Competition 4 dataset 2a. $M = 125$ samples. Channel C3. Left hand movement.

III. RESULTS

The proposed framework is tested on the BCI Competition 4 dataset 2a [18]. The cue–based BCI paradigm consisted of four motor imagery tasks. For this study, we focused on classes 1 and 2 (left and right hand movement, respectively) of the first session. Data from every subject (9 in total) comprised of 72 trials per class, 22 Ag/AgCl EEG recording channels sampled at 250 Hz and bandpassed between 0.5 Hz and 100 Hz.

Each trial consisted on a visual cue determining the beginning of the motor imagery task. Each subject was instructed to perform the requested movement for 6 seconds until the visual cue disappeared. For the current analysis, we extracted 4–second–long segment corresponding to 2 seconds before and after movement cue. A 5-th order Butterworth filter with 3 dB cut–off frequencies of 8 Hz and 35 Hz was used to isolate the mu and beta rhythms.

Each ensemble of bandpassed, single–channel, multi–trial recordings (per task) are mapped to their corresponding β_M spaces and subsequently non–linearly separated into background and phasic event components. A value of $M = 125$ samples (0.5 sec.) is utilized to capture the scale–specific nature of the rhythms of interest. The first set of results showcases the shifts in dynamics around movement cue. Particularly, we estimate the average number of wave packets before and after visual cue for 2–second intervals. Then, the difference between pre and post estimates is calculated for each channel. Fig. 2 shows the topographical distribution of the phasic event rates difference for two subjects. The mirroring effect resembles the contralateral ERS and ipsilateral ERD of the central sensorimotor rhythm [10]; yet, the estimates are not the result of amplitude–based encoding, but rather of rate–based encoding at a mesoscopic level.

Next, the effective compression rate of the system is estimated. Let N and $\hat{N}$ be the number of non–zero discrete time samples in $\tilde{y}[n]$ and $\hat{y}[n]$, respectively. The rate, K, is simply equal to $\frac{\hat{N}}{N}$ and determines the fraction of samples preserved in $\hat{y}[n]$ by the non–linear filtering scheme. Then, average ℓ_2–norms from the M–snippets corresponding to phasic event and background components are estimated per
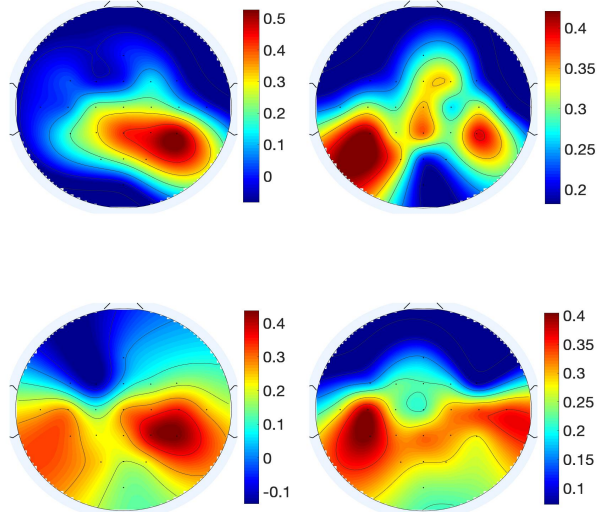

Fig. 2. Topographical distribution of wave packet rates difference (measured in neuromodulations per second) after non–linear source separation via the Discriminative Embedding Transform. Top row: Subject 1. Bottom row: Subject 7. Left and right columns correspond to left and right hand movement, respectively.

channel. Logarithms of the differences constitute the features. The 22–dimensional feature vectors are projected to a one–dimensional subspace via Linear Discriminant Analysis (LDA). The separability of both classes in this lower dimensional space is determined exploiting a well known measure in unsupervised learning—the average Silhouette value [19]. Particularly for the i-th point, its Silhouette S_i, is defined as:

$$S_i = \frac{b_i - a_i}{\max\{a_i, b_i\}} \qquad (6)$$

where b_i is the average Euclidean distance of i to all points in the cluster where i is not a member, and a_i is the average distance between i and all the points in the same cluster. S_i is bounded between -1 (poor clustering solution) and 1 (high separability between classes). Similarly, the average Silhouette value is estimated for the features computed from the original, bandpassed EEG traces, $\tilde{y}[n]$. To allow fair comparisons, we estimated the log–variance using only the 2–second–long segments after visual cue, i.e. the equivalent compression rate of the filtered EEG is $K = 0.5$.

Fig. 3 summarizes the relationship between separability of motor imagery classes and compression rate for all 9 subjects in the dataset. Most of the cases display a compression rate around 0.05, i.e. in average, less than 5% of the samples in the multivariate time series are needed to achieve high discriminability between tasks. The grand average Silhouette value for the phasic event components is 0.46, while the filtered traces achieve a mean of 0.39. Thus, the proposed framework produces higher separabilities with significantly less data. This confirms the discriminant and sparse nature of the wave packets in the EEG.
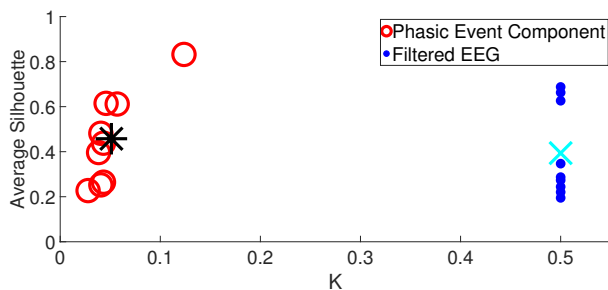
Fig. 3. Average Silhouette values versus compression rate for all subjects. Red circles and blue dots represent measures derived from wave packets and filtered EEG, respectively. Black (0.05, 0.46) and cyan (0.5, 0.39) marks indicate grand averages over subjects.

Fig. 3 also suggests that the proposed framework is a data–driven source selector—it implicitly selects which channels are more *active* during the task and isolates the relevant M–snippets accordingly. Yet, this statement must be taken with a grain of salt because the selection is solely based on the rhythm under study. The remaining rhythms might be correlated to the task in other ways we are not quantifying.

Lastly, we investigated the effect of the M parameter over the average separability between classes and compression rate. As Table I indicates, the compression rate, K, monotonically increases with M, i.e. when the M–snippets grow in dimensionality. On the other hand, the average discriminability between motor tasks seems fairly stable. This suggests the proposed algorithm is robust for a suitable and neurophysiologically principled interval of M.

TABLE I
GRAND AVERAGE SILHOUETTE VALUE AND COMPRESSION RATE AS A FUNCTION OF EMBEDDING TRANSFORM FREE PARAMETER, M.

	M (s.)				
	0.40	0.45	0.50	0.55	0.60
Silhouette	0.462	0.474	0.458	0.466	0.467
K	0.050	0.050	0.051	0.053	0.054

IV. CONCLUSION

We proposed a non–linear source separation framework to isolate scale–specific wave packets from bandpassed single–channel, multi–trial EEG recordings. The Embedding Transform followed by non–linear mode separation allows to preserve the discriminant signatures of the traces in a data–driven scheme fully based on neurophysiological principles. An EEG–based BCI showcases the potential of the non–linear mechanism by achieving higher discriminability measures than whole, filtered EEG traces. The algorithms are also robust and fairly insensitive to the only free parameter of the model.

In the future, we will analyze in depth the constraints for optimal mode separation in the β_M domain; for instance γ for Subject 9 in Fig. 1 is clearly biased. This is most likely due to the inherent dynamics of the traces or a consequence of a parametric Gaussian mixture fitting. Additionally, EEG is a complex, non–linear, high–dimensional, multivariate time series and, as such, can benefit from frameworks focused on compression rates and high bandwidths, e.g. compressed sensing, sparse coding, and lossy compression. Future work can harness the principles from those fields and formally define a compression framework for the EEG where only discrete events highly correlated to physiological processes or external stimuli are encoded.

REFERENCES

[1] E. Niedermeyer and F. L. da Silva, *Electroencephalography: basic principles, clinical applications, and related fields*. Lippincott Williams & Wilkins, 2005.

[2] A. Rechtschaffen, A. Kales, L. A. B. I. S. University of California, and N. N. I. Network, *A Manual of Standardized Terminology, Techniques and Scoring System for Sleep Stages of Human Subjects*, ser. Publication. Brain Information Service/Brain Research Institute, University of California, 1968.

[3] F. Mormann, K. Lehnertz, P. David, and C. E. Elger, "Mean phase coherence as a measure for phase synchronization and its application to the EEG of epilepsy patients," *Physica D: Nonlinear Phenomena*, vol. 144, no. 3-4, pp. 358–369, 2000.

[4] A. A. Handojoseno, J. M. Shine, T. N. Nguyen, Y. Tran, S. J. Lewis, and H. T. Nguyen, "Analysis and prediction of the freezing of gait using EEG brain dynamics," *IEEE transactions on neural systems and rehabilitation engineering*, vol. 23, no. 5, pp. 887–896, 2015.

[5] M. A. Lebedev and M. A. Nicolelis, "Brain–machine interfaces: past, present and future," *TRENDS in Neurosciences*, vol. 29, no. 9, pp. 536–546, 2006.

[6] A. Kübler, B. Kotchoubey, J. Kaiser, J. R. Wolpaw, and N. Birbaumer, "Brain–computer communication: Unlocking the locked in." *Psychological bulletin*, vol. 127, no. 3, p. 358, 2001.

[7] J. R. Wolpaw, N. Birbaumer, D. J. McFarland, G. Pfurtscheller, and T. M. Vaughan, "Brain–computer interfaces for communication and control," *Clinical neurophysiology*, vol. 113, no. 6, pp. 767–791, 2002.

[8] J. R. Wolpaw and D. J. McFarland, "Control of a two-dimensional movement signal by a noninvasive brain-computer interface in humans," *Proceedings of the national academy of sciences*, vol. 101, no. 51, pp. 17 849–17 854, 2004.

[9] G. Pfurtscheller, C. Brunner, A. Schlögl, and F. L. Da Silva, "Mu rhythm (de) synchronization and EEG single-trial classification of different motor imagery tasks," *NeuroImage*, vol. 31, no. 1, pp. 153–159, 2006.

[10] G. Pfurtscheller and F. L. Da Silva, "Event-related EEG/MEG synchronization and desynchronization: basic principles," *Clinical neurophysiology*, vol. 110, no. 11, pp. 1842–1857, 1999.

[11] G. Buzsaki, *Rhythms of the Brain*. Oxford University Press, 2006.

[12] W. Freeman and R. Q. Quiroga, *Imaging brain function with EEG: advanced temporal and spatial analysis of electroencephalographic signals*. Springer Science & Business Media, 2012.

[13] N. Hazarika, J. Z. Chen, A. C. Tsoi, and A. Sergejew, "Classification of EEG signals using the wavelet transform," in *Digital Signal Processing Proceedings, 1997. DSP 97., 1997 13th International Conference on*, vol. 1. IEEE, 1997, pp. 89–92.

[14] S. Sanei and J. A. Chambers, "EEG signal processing," 2007.

[15] C. A. Loza and J. C. Principe, "The embedding transform. a novel analysis of non-stationarity in the EEG," in *Engineering in Medicine and Biology Society (EMBC), 2018 IEEE 40th Annual International Conference of the*. IEEE, 2018, pp. 3112–3115.

[16] B. W. Jervis, M. J. Nichols, T. E. Johnson, E. Allen, and N. R. Hudson, "A fundamental investigation of the composition of auditory evoked potentials," *IEEE Transactions on Biomedical Engineering*, no. 1, pp. 43–50, 1983.

[17] C. A. Loza, M. S. Okun, and J. C. Príncipe, "A marked point process framework for extracellular electrical potentials," *Frontiers in systems neuroscience*, vol. 11, p. 95, 2017.

[18] M. Tangermann, K.-R. Müller, A. Aertsen, N. Birbaumer, C. Braun, C. Brunner, R. Leeb, C. Mehring, K. J. Miller, G. Mueller-Putz, *et al.*, "Review of the BCI competition IV," *Frontiers in neuroscience*, vol. 6, p. 55, 2012.

[19] P. J. Rousseeuw, "Silhouettes: a graphical aid to the interpretation and validation of cluster analysis," *Journal of computational and applied mathematics*, vol. 20, pp. 53–65, 1987.